Electronic Supplementary Material (ESI) for Journal of Materials Chemistry C.

Supporting Information

Chiral Nematic Mesoporous Magnetic Ferrites

Georg R. Meseck[a], Andrea S. Terpstra[a], Armando J. Marenco[b], Simon Trudel[b]*, Wadood Y. Hamad[c], Mark J. MacLachlan[a]*

[a] Department of Chemistry, University of British Columbia, 2036 Main Mall, Vancouver, BC, V6T 1Z1, Canada

[b] Department of Chemistry and Institute for Quantum Science and Technology, University of Calgary, 2500 University Drive NW, Calgary, AB, T2N 1N4, Canada.

[c] FPInnovations, 2665 East Mall, Vancouver, BC, V6T 1Z4, Canada

Email: mmaclach@chem.ubc.ca; trudels@ucalgary.ca

Table of Contents

1 EXPERIMENTAL

1.1 MATERIALS

Iron(III) nitrate nonahydrate and copper(II) nitrate hemipentahydrate were purchased from Fisher Scientific. Nickel(II) nitrate hexahydrate and cobalt(II) nitrate hexahydrate were purchased from Sigma Aldrich. All solvents and tetramethyl orthosilicate (TMOS, Acros) were used without further purification. A solution of cellulose nanocrystals (CNCs) of (195±93) nm in length and (15±8) nm in width (determined by TEM) at a pH of 2.5 was supplied from FPInnovations.

1.2 MAGNETOMETRY

Superconducting quantum interference device (SQUID) magnetometry measurements were performed using a Quantum Design MPMS XL-7S system. Nanoparticles (NPs) were loaded into a gelatin capsule, sealed with Kapton tape, and inserted in a diamagnetic clear plastic straw. Thin-films measurements were performed with the sample loaded in a longitudinal or transverse fashion in reference to the applied external magnetic field. For longitudinal measurements, films were secured to a quartz road with GE 7031 varnish diluted in a 1:1 ratio with isopropyl alcohol. For transverse measurements, films were sandwiched between two plastic straw cutouts and sealed with GE varnish. This "puck" was then loaded into a diamagnetic clear plastic straw held in place by plastic straw adapters.

Isothermal magnetization as a function of magnetic field strength measurements were carried out at 300 K by cycling the applied field between 4 and -4 T. Zero-field-cooled (ZFC) and field-cooled (FC) magnetization measurements were carried out by cooling samples to 1.9 K in the absence (ZFC) or presence (FC) of an applied magnetic field of 10 mT, and measuring the magnetization under a field of 10 mT upon warming the sample. M(H) measurements to a maximum magnetic field strength of 7 T were carried out to obtain M_s.

1.3 SCANNING ELECTRON MICROSCOPY

Scanning electron micrographs were acquired on a Hitachi S4700 cold field emission microscope at an acceleration voltage of $U = 2.3$ kV and a beam current of $I = 10$ µA. The samples were sputter coated with 6 nm of Pt/Pd (80/20) using a Cressington 208C high resolution sputter coater prior to imaging.

1.4 NITROGEN ADSORPTION

N_2 adsorption isotherms were measured using a Micromeritics ASAP 2020 at 77 K. All samples were degassed under vacuum at 110 °C immediately prior to analysis. BET (Brunauer, Emmett and Teller) theory

was used to determine surface areas and BJH (Barrett-Joyner-Halenda) pore size distributions were all calculated from the adsorption branch of the isotherm.

1.5 Powder X-ray Diffraction (PXRD)

Powder X-ray diffractograms were collected on a Bruker D8 Advance diffractometer using CuK_α as the X-ray source and a NaI scintillation detector. Crystallite sizes were determined from the integral breadth of non-overlapping peaks using the EVA software package (Bruker).

1.6 Energy Dispersive X-ray Spectroscopy (EDX)

For EDX analysis samples were finely ground and the resulting powder mounted on an aluminum sample holder using an adhesive carbon tab. Spectra were acquired on a Hitachi S-2600N at an acceleration voltage of $U = 16$ kV and fitted using the Quartz Imaging Systems XOne software package before calculating the concentrations from the K_α lines.

1.7 Preparation of Chiral Nematic Mesoporous Silica (CNMS)

CNMS was prepared according to a modified literature procedure.[1] The CNC suspension was diluted to the desired concentration (4 wt. %). TMOS was added dropwise to a CNC suspension (1.69 mmols TMOS / 150 mg of CNC) and stirred at room temperature for 2 hours. The CNC/TMOS mixture was then transferred to polystyrene Petri dishes (20 mL / 90 mm dish) and left to dry under ambient conditions over two days forming CNC/silica composite films. The CNC/silica composite films were placed in 6 M H_2SO_4 (~250 mg / 500 mL) and heated to 100 °C for 18 h. After cooling to room temperature and filtering, the films were washed with Piranha solution yielding free standing CNMS films.

1.8 Hard Templating of Ferrites

CNMS (200 mg) was passed through a sieve with 30 µm mesh size to obtain a powder, then given into a polypropylene beaker. Solutions of the respective metal nitrate (333 µL, 0.8 M in ethanol) and iron nitrate (666 µL, 0.8 M in ethanol) were premixed and then added dropwise onto the silica. After 2 h at room temperature the evaporation of the solvent was completed by placing the beaker on a hot plate and setting the temperature to $T = 100$ °C for 4 h. The nitrate precursors were subsequently decomposed under air by heating the material to $T = 200$ °C for 3 h (ramp $\Delta T = 1$ °C min^{-1}). This procedure was typically repeated three times; i.e. until nitrogen adsorption showed a decrease of accessible pore volume > 60 %. After calcination at the desired temperature for 4 h (ramp $\Delta T = 2.5$ °C min^{-1}) the silica matrix was etched by immersing the sample in sodium hydroxide solution (0.25 mL mg^{-1}, 2 M). The material was gently washed by exchanging the solution repeatedly with DI water using a pipette. After repeating the washing procedure with ethanol the material was left to dry under ambient conditions.

2 SUPPORTING CHARACTERIZATION

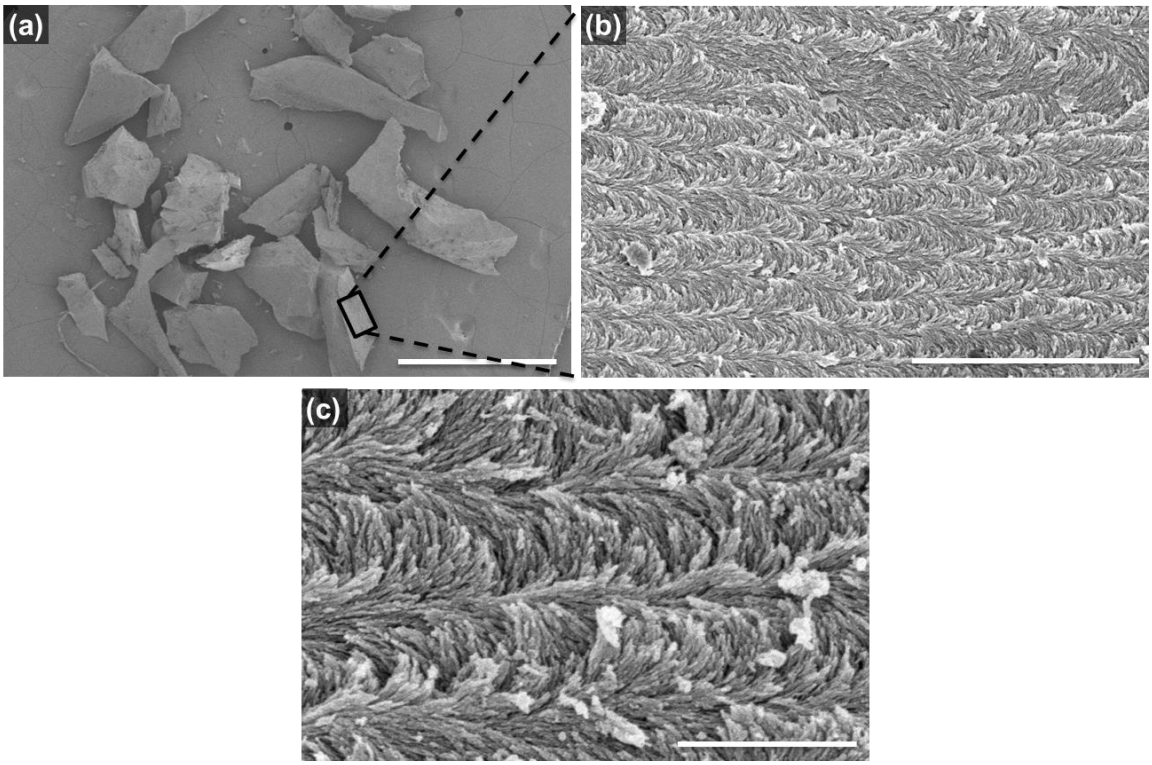

Figure S1. Scanning electron micrographs of CNMS powders which were used as template for the ferrite material show the chiral nematic structure on a cross-section of the silica film. Scale bars: (a) 1 mm; (b) 5 µm; (c) 1 µm.

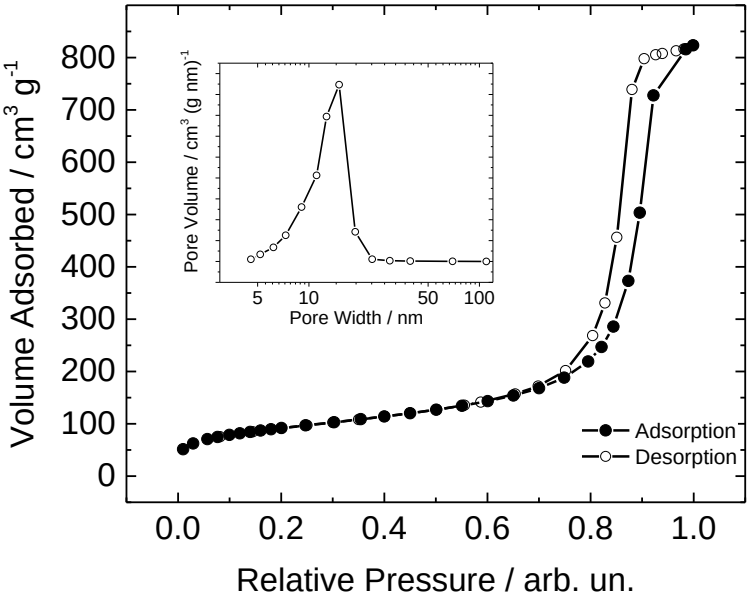

Figure S2. Nitrogen adsorption-desorption isotherm data for a batch of CNMS powder which was used as template with a BET surface area of 309 m^2/g. Inset shows BHJ pore size distribution of 16-19 nm.

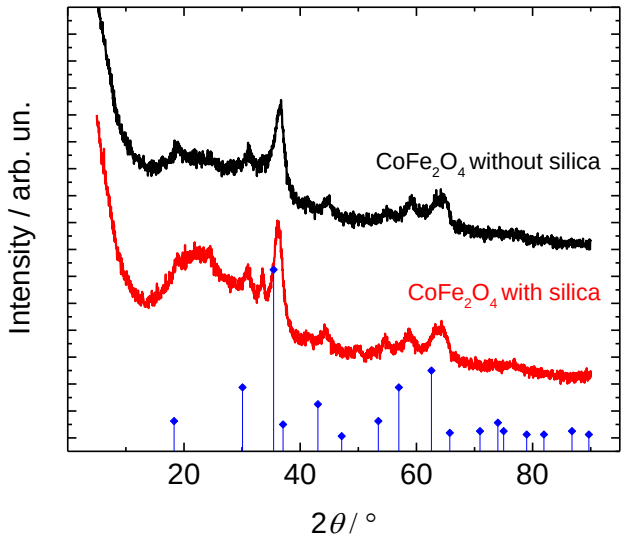

Figure S3 PXRD data of cobalt ferrite after thermal decomposition at $T = 200$ °C shows low crystallinity. Composite materials (red) and after removal of the silica matrix (black).

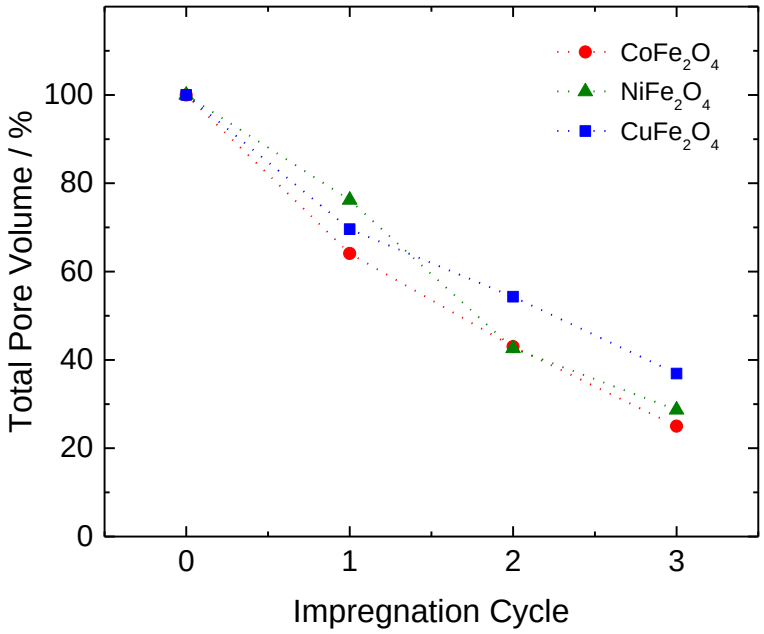

Figure S4. Nitrogen adsorption-desorption isotherm data shows a decrease in the total pore volume of the cobalt, nickel and copper ferrites with each impregnation cycle.

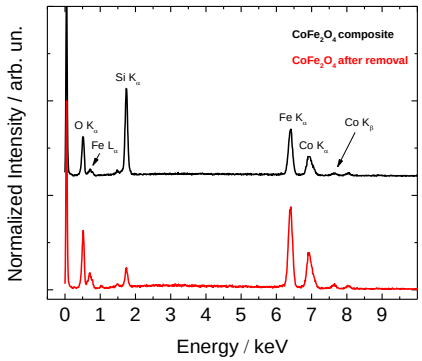

Element	Concentration / wt%	
	Composite	After removal
Carbon	10	8
Oxygen	25	17
Silicon	16	2
Iron	31	47
Cobalt	18	26

Figure S5 EDX data for cobalt ferrite (calcined at T_{calc} = 600 °C) shows removal of the silica matrix by etching in sodium hydroxide.

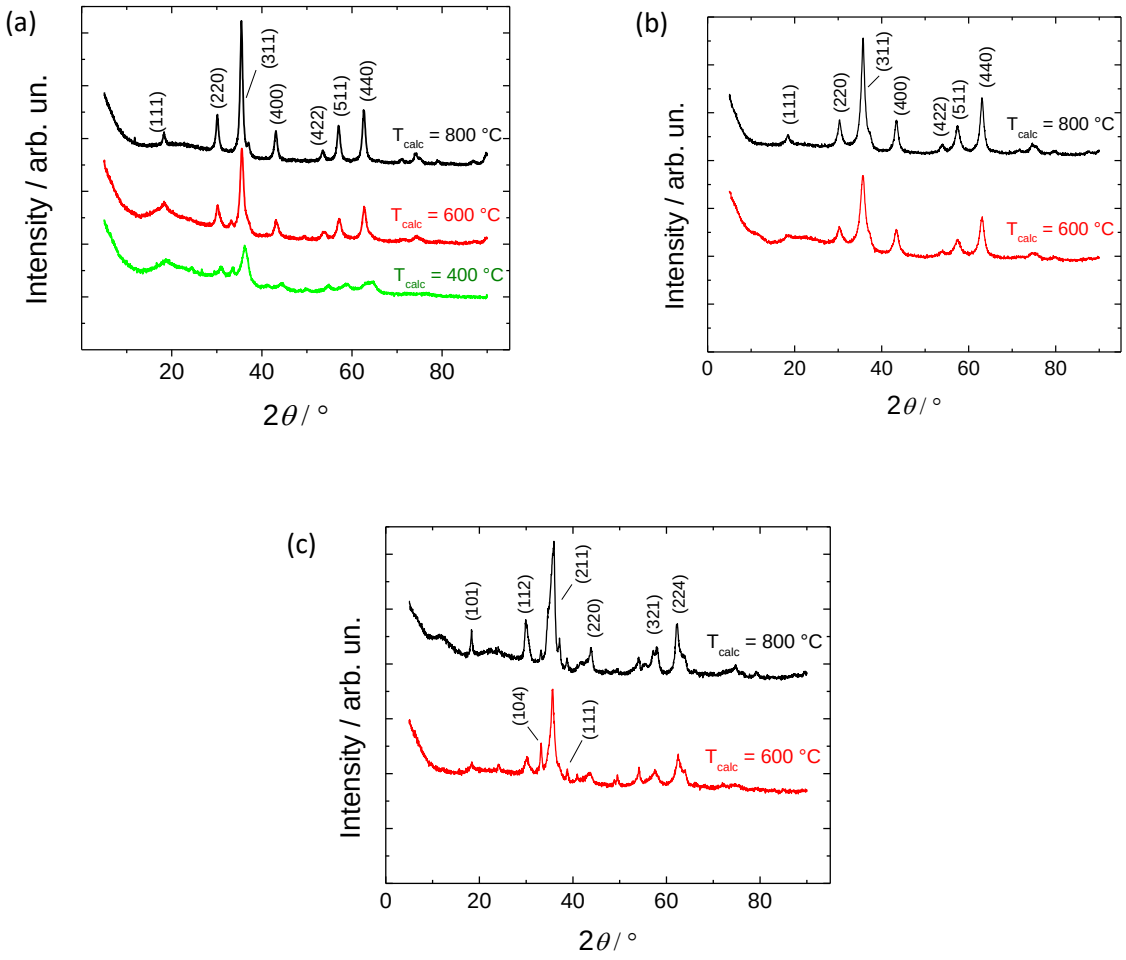

Figure S6. PXRD data of ferrite samples for (a) Cobalt ferrite calcined at T_{calc} = 400 °C, 600 °C and 800 °C (matched to PDF card: 00-022-1086), (b) nickel ferrite calcined at 600 °C and 800 °C (matched to PDF card: 01-076-6119) and (c) copper ferrite calcined at 600 °C and 800 °C (matched to PDF card: 00-034-0425) with (104) identifying strongest hematite peak and (111) identifying trace copper oxide peak.

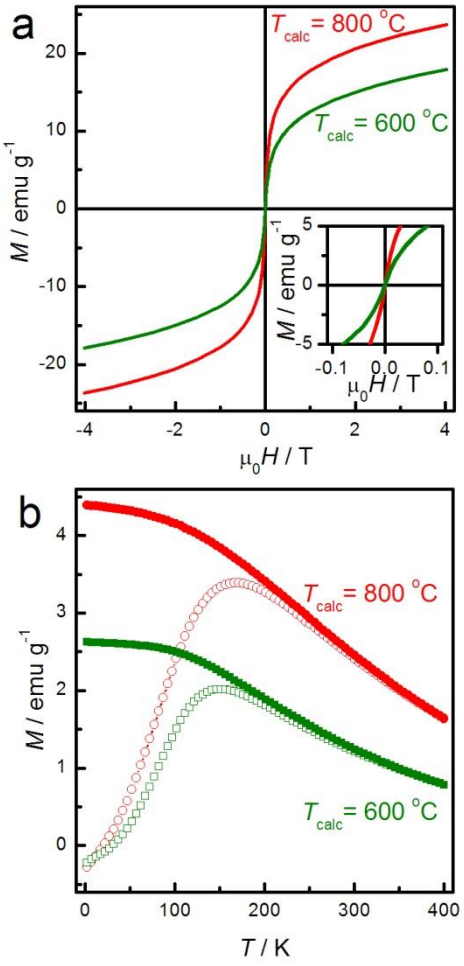

Figure S7. SQUID magnetometry measurements of $NiFe_2O_4$ NPs calcined at T_{calc} = 600 and 800 °C. (**a**) Magnetic hysteresis loops at 300 K including a zoomed-in area near the origin (inset). (**b**) ZFC-FC measurements ($\mu_0 H$ = 10 mT) (open symbols: ZFC; solid symbols: FC).

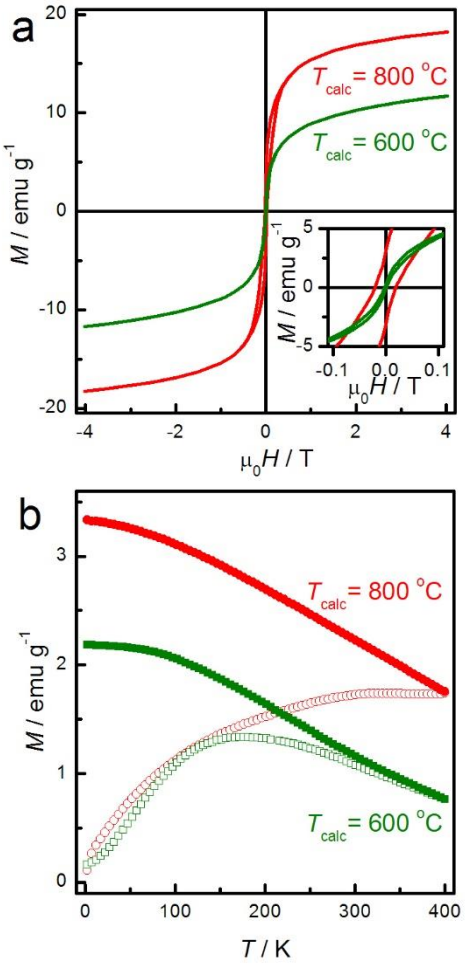

Figure S8. SQUID magnetometry measurements of $CuFe_2O_4$ NPs calcined at 600 and 800 °C. (**a**) Magnetic hysteresis loops at 300 K including a zoomed-in area near the origin (inset). (**b**) ZFC-FC measurements ($\mu_0 H$ = 10 mT) (open symbols: ZFC; solid symbols: FC).

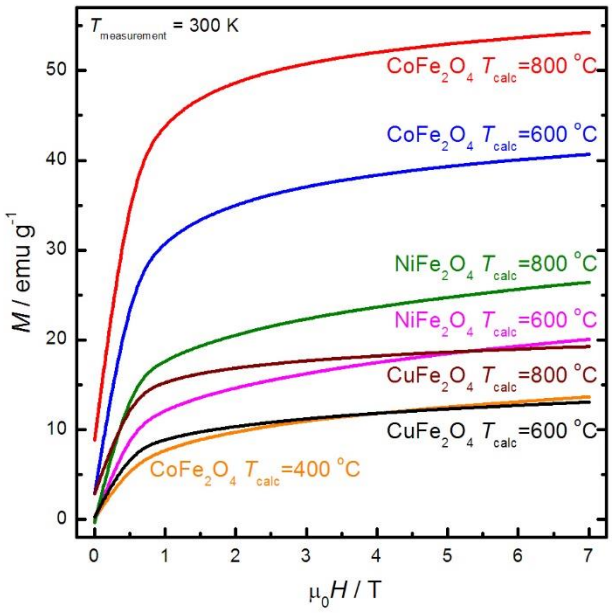

Figure S9. M(H) at 300 K for spinel ferrites to a maximum magnetic field of 7 T to determine M_S. T_{calc} corresponds to the calcination temperature for the sample.

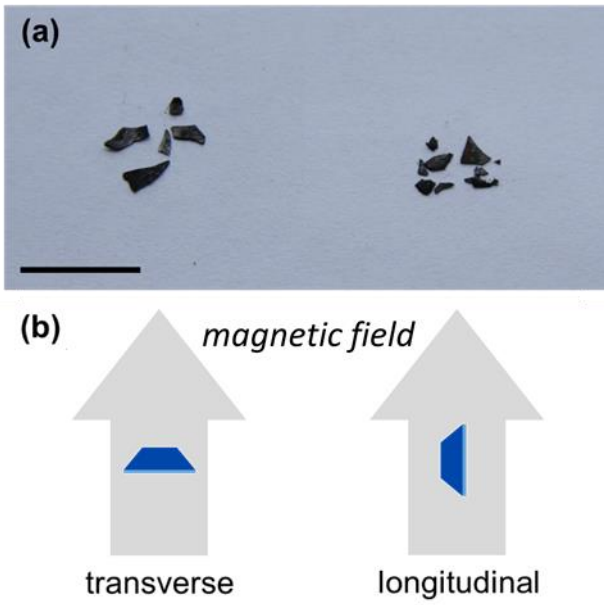

Figure S10. (**a**) Photographs of $CoFe_2O_4$ / silica film (left) and $CoFe_2O_4$ film calcined at 600 °C; scale bar 10 mm. (**b**) Illustration of transverse and longitudinal alignment of the films for SQUID magnetometry.

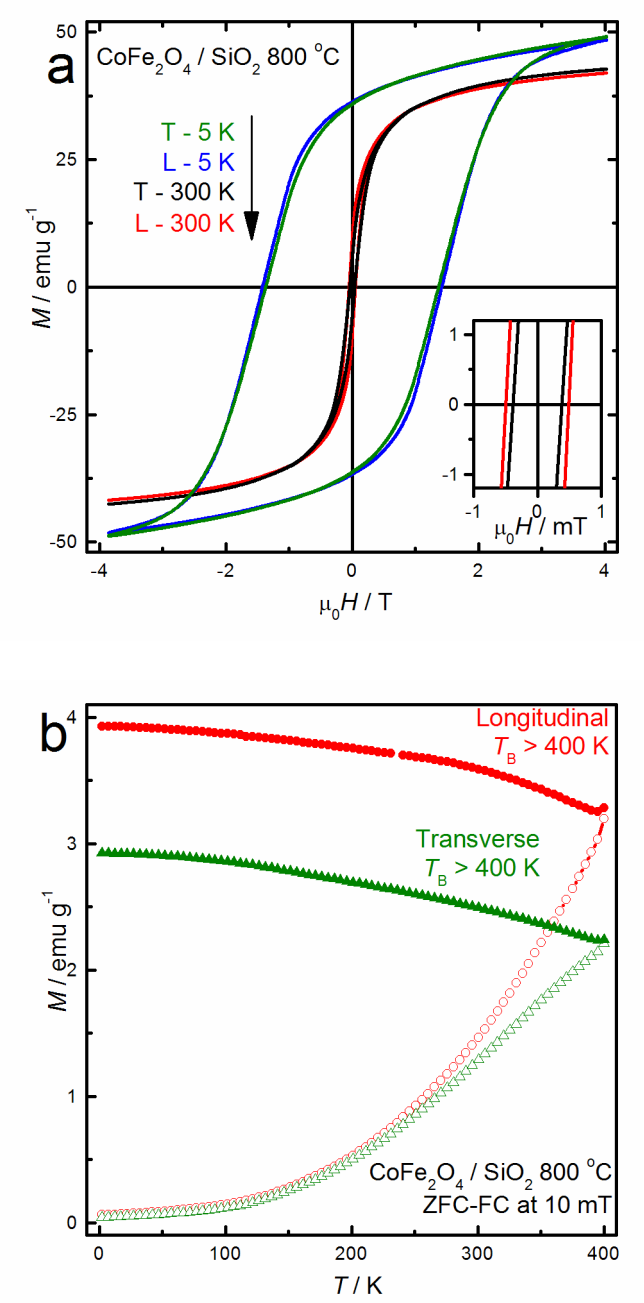

Figure S11. SQUID magnetometry measurements of $CoFe_2O_4$ / silica film calcined at T_{calc} = 800 °C. (**a**) Magnetic hysteresis loops at 5 and 300 K for longitudinal (L) and transverse (T) alignment of the film with the magnetic field including a zoomed-in area near the origin (inset). (**b**) ZFC-FC measurements ($\mu_0 H$ = 10 mT) (open symbols: ZFC; solid symbols: FC).

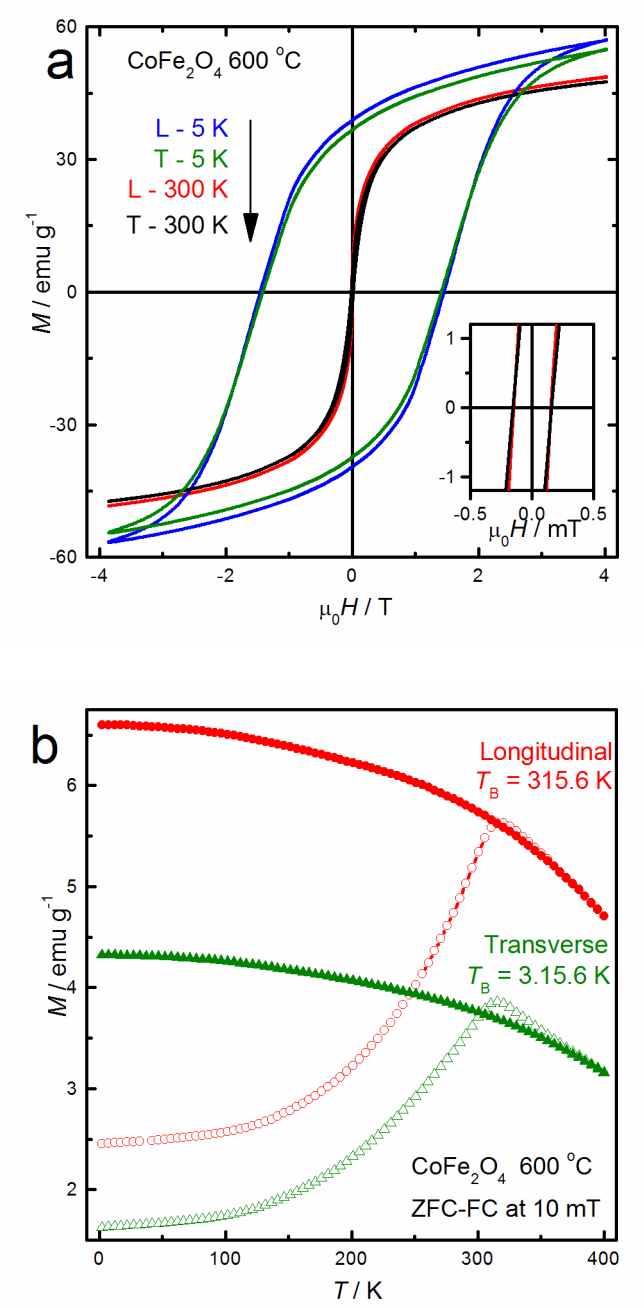

Figure S12. SQUID magnetometry measurements of $CoFe_2O_4$ film calcined at T_{calc} = 600 °C. (**a**) Magnetic hysteresis loops at 5 and 300 K for longitudinal (L) and transverse (T) alignment of the film with the magnetic field including a zoomed-in area near the origin (inset). (**b**) ZFC-FC measurements ($\mu_0 H$ = 10 mT) (open symbols: ZFC; solid symbols: FC).

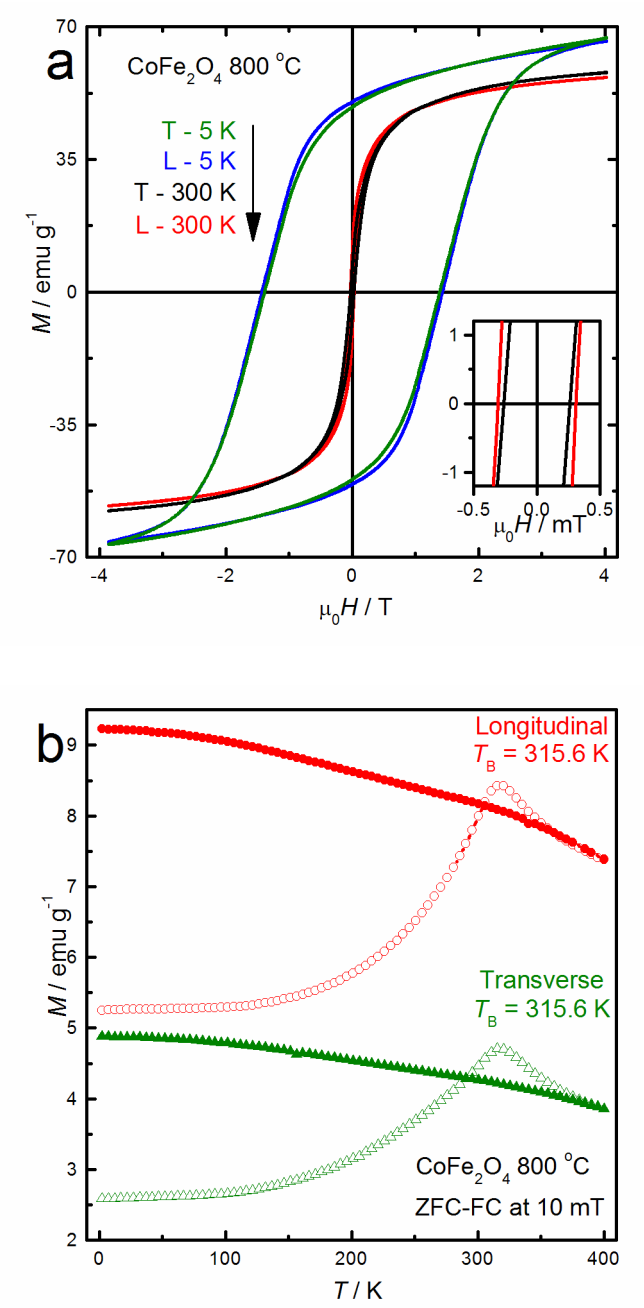

Figure S13. SQUID magnetometry measurements of $CoFe_2O_4$ film calcined at T_{calc} = 800 °C. (**a**) Magnetic hysteresis loops at 5 and 300 K for longitudinal (L) and transverse (T) alignment of the film with the magnetic field including a zoomed-in area near the origin (inset). (**b**) ZFC-FC measurements ($\mu_0 H$ = 10 mT) (open symbols: ZFC; solid symbols: FC).

Table S1. Material properties of ferrite replicas and magnetic properties of ferrite NPs.

Calcination T_{calc} / °C	M_s @ 7 T / emu g^{-1}	M_s @ 4 T / emu g^{-1}	M_r/M_s ($\mu_0 H_{max}$ = 4 T)	$\mu_0 H_c$ / mT ($\mu_0 H_{max}$ = 4 T)	T_B / K	K_{eff} / kJ m^{-3}	Crystallite Size / nm	Surface Area / m^2 g^{-1}	Pore Size / nm	Pore Volume / cm^3
Cobalt ferrite, $CoFe_2O_4$										
400	13.6	11.2	0.02	1.73	241	606	6.4	122	19	0.60
600	40.7	37.9	0.10	10.6	> 400	> 415	8.6	76	28	0.53
800	54.3	52.0	0.17	33.1	> 400	> 221	10.6	52	33	0.44
Nickel ferrite, $NiFe_2O_4$										
600	20.1	17.9	6.55×10^{-3}	1.00	151	317	6.8	139	24	0.85
800	26.4	23.7	8.60×10^{-3}	0.86	166	189	8.2	112	26	0.73
Copper ferrite, $CuFe_2O_4$										
600	13.1	11.7	0.02	1.91	176	210	8.2	106	27	0.81
800	19.3	18.3	0.16	19.9	> 400	> 289	9.7	57	29	0.41